Journal of Ceramic Processing Research. Vol. 22, No. 3, pp. 323~328 (2021)
(Received 5 October 2020, Received in revised form 21 December 2020, Accepted 29 December 2020)
https://doi.org/10.36410/jcpr.2021.22.3.323

J O U R N A L O F
Ceramic Processing Research

Physical and mechanical properties of low-temperature glass-ceramics from waste glass cullet and Class C-fly ash

Pattarasuda Viensiri, Suthee Wattanasiriwech and Darunee Wattanasiriwech*
Center of Innovative Materials for Sustainability, School of Science, Mae Fah Luang University, Thailand

CAS ($CaO–Al_2O_3–SiO_2$) glass-ceramic was prepared from class C fly ash (FA) and the powdered waste glass (PWG) in the weight ratio of FA: PWG = 40: 60 (denoted as F40) and sintered in a single-stage at 700-1,000 ºC. X-ray diffraction (XRD) analysis showed that the crystallization of the mixture into wollastonite, augite, and zeolite had occurred after sintering. Microscopically investigation showed acicular type crystals distributing on the glassy matrix of the F40, in correspondence to the XRD result. The F40 showed promising Vickers hardness and flexural strength with the maximum values of 7.4 GPa and 57.6 MPa respectively. Further attempt to improve the mechanical property of the obtained glass-ceramics using the two-stage sintering profiles was achieved with the respective maximum hardness and flexural strength of 8.2 GPa and 62.5 MPa. The result showed that the prepared CAS glass-ceramics were suitable for use as low water absorption tiles according to the Thai Industrial Standard for Ceramic Tiles (TIS 2508-2555). The superior physical and mechanical properties as well as the low firing temperature opened the opportunity for waste management by up-cycling as a new building material.

Keywords: Glass-ceramic, Fly ash, Glass cullet, Flexural strength, Vickers hardness.

Introduction

The term glass-ceramics refers to a material that combines between glasses and polycrystalline ceramics via controlled nucleation and crystallization [1]. Internal or external nucleation is promoted to develop micro-heterogeneities from which crystallization can subsequently begin [2]. Glass-ceramics have a wide range of applications from construction (building and decoration), dental and medical, to waste removal due to the outstanding mechanical properties, chemical resistance, and immobilization stability of heavy metals [3-6]. A typical microstructure of the glass-ceramic contained a high fraction of the crystalline phases, with the remaining being glass. In this aspect, the properties of the final product can be tailor-designed by a selection of the crystal types and contents along with the adjustment of the glass matrix composition. For example, leucite reinforced ceramics for dental porcelain may contain between 17 and 41 wt% of leucite [7] with biaxial flexural strengths varying from 56 to 137 MPa [8].

Glass-ceramics are typically prepared from the parent glass via the control of the crystallization process. Convention technique involved the heating in two stages which are, nucleation and crystallization. Another technique is called one-stage, where a nucleating agent is incorporated in order to narrow the temperature gap between the nucleation and crystallization [5]. Solid waste with a complex composition was reported to be an effective nucleation agent but with a more unclear mechanism than using the pure compounds [6].

Waste-derived materials have been gaining attention due to the constrain in landfill space occupancy and the concern on depletion of natural resources. Glass-ceramic is one of the target products due to its versatile applications [9, 10]. The high contents of fluxing substances in these waste materials allowed the sintering to occur at the low temperature, making it beneficial for energy and cost-saving [11]. Fly ash, a by-product of coal combustion, was one of the raw materials used for glass-ceramic making due to its high contents in glass composition [12]. The glass-ceramics prepared from coal fly ash normally fall in the $CaO–Al_2O_3–SiO_2$(CAS) system, which combines good mechanical properties (bending strength and abrasion resistance) and chemical stability, making them suitable for their main application in the construction industry [13]. Previously wollastonite glass-ceramic with optimum mechanical properties had been reported [14]. The experiment, however, involved with the melting of the components at 1400°C for 3 hrs., quenching and grinding before forming and heat treating at 1,000 ºC and 1,050 ºC. Another work on waste glass incorporated fly ash showed microhardness value as high as 3,833 HV due to a higher degree of densification/consolidation when waste glass percentage was increased to 15% [15]. The work, however, did not conduct the strength test. It was reported that fly ash blended with window glass and calcium fluoride (CaF_2) showed an improved strength when cerium oxide (CeO_2)

*Corresponding author:
Tel : +6653916263
Fax: +6653916776
E-mail: darunee@mfu.ac.th

was added [16]. The processing steps involved typical glass-ceramic making which was melting the components, quenching, and heating again.

In this research, our further attempt to use the mixed municipal waste glass cullet as the precursor material for the preparation of a low-temperature glass-ceramic for a construction purpose was addressed. Glass is a closed-loop material, i.e. it can be fully recycled. Practically, however, glass recycling occurs at a lower percentage due to the limitation of the recycling process and local management policy [17, 18]. Waste glass, thus, has become an environmental concern due to its landfill space occupancy. The composition of the precursor material was experimentally adjusted to be suitable for obtaining glass-ceramic by incorporating Class C-fly ash. Sintering was performed in two main scenarios; one stage and two stage-sintering. The physical and mechanical properties of the products were examined and compared to the Thai Industrial Standard for Ceramic Tiles (**TIS 2508-2555**).

Materials and Methods

Material preparation

The municipal waste glass was collected and pre-treated according to ref. [19]. After crushing with the hammer mill, the glass cullet was ball-milled for 3 hrs before size-screening using a #200 mesh-sieve. The resulting powdered waste glass (PWG) had a particle size of <75 μm. Class-C fly ash (FA) was received from Mae Moh Power Plant, Lampang, Thailand. The chemical compositions of the FA and PWG are shown in Table 1. Analysis of the FA was reported elsewhere [20]. The analysis showed the existence of $CaSO_4$, quartz, and iron oxide on the amorphous background.

Fly ash (FA) was mixed with the powdered waste glass (PWG) at the weight ratio of 40:60 (denoted as F40) and ball milled for another 4 hrs. The mixed powder was then compacted at a pressure of 100 MPa with an aid of 0.4% PVA binder solution. The compacted samples were sintered with a heating rate of 5 °C/min at 700-1,000 °C for 1 hr before being naturally cooled in the furnace to room temperature.

The samples were performed with the 2-stage sintering to enhance the crystallization process. The scheme was done in two scenarios; (a) holding at the nucleation temperature before further increasing to the densification temperature at 1,000 °C and (b) holding at lower temperature after the peak densification temperature. The sintering profile and the sample code is displayed in Table 1. Noted that the heating and cooling rate are fixed at 5 °C/min to the assigned temperatures.

Table 1. The two-stage sintering profiles.

Sample Code	Step 1		Step 2	
	Temperature (°C)	Holding time (min)	Temperature (°C)	Holding time (min)
Tn700	700	30	1000	60
Tn750	750	30	1000	60
Tc850	1000	60	850	60
Tc900	1000	60	900	60
Tc950	1000	60	950	60

Characterization and testing

Density, porosity, and water absorption were measured following ASTM C373-14a. Surface morphology of the surface was observed using a scanning electron microscopy (SEM, LEO 1450 VP) at an accelerating voltage of 20 kV. The surface was polished etched using 4% HF for 30 sec. Phase development was monitored using an X-ray diffraction instrument (XRD, PANalytical, X'pertPro) and the software X'pert High Score Plus (X'pertPro MPD Philip, Netherlands). The sample was etched with a 4% HF solution for 2 min before the microscopical investigation. The flexural strength, measured using a ball on ring technique, was investigated and calculated according to Eq. (1).

$$\sigma_{max}=\frac{3P(1+\nu)}{4\pi t^2}\left[1+2\ln\frac{a}{b}+\frac{(1-\nu)}{(1+\nu)}\left\{1-\frac{b^2}{2a^2}\right\}\frac{a^2}{R^2}\right] \quad (1)$$

where P = load (N), t = disk thickness (mm), a = radius of the circle of support points (mm), b = radius of the region of uniform loading at the center (mm), R = radius of the disk (mm), v = Poisson's ratio.

The Vickers hardness averaged from 5 points was measured using a microhardness indentation method (Matsuzawa MMT-3 type F) at a load of 2945 mN and was calculated according to Eq. (2).

$$H=\frac{1.8P}{a^2} \quad (2)$$

where H = Vickers hardness (MPa), P = test load in Vickers hardener (MPa), a = half average length of the diagonal of the Vickers marks (microns).

Results and Discussion

The X-ray diffraction analysis of the F40 fired at different temperatures is shown in Fig. 1. The F40 fired from 700-1,000 °C showed the existence of 3 crystalline phases; wollastonite [$CaSiO_3$], augite [$Ca(Mg,Al)Si_2O_6$] and zeolite [$Na_3Ca_4Si_{12}Al_{12}O_{48}(I_2)_{5.52}$]. The crystalline peaks were more intensified with increasing firing temperatures indicating progressive crystallization. The previous work showed that wollastonitic glass-ceramics (WGCs) could be prepared through vitrification of medical wastes incinerator fly ash (MFA) with soda lime recycled glass (SLRG) at 1,300 °C, followed by re-crystallization in the range of 950 °C [4]. CaO-MgO-Al_2O_3-SiO_2 glass-ceramics with diopside as the

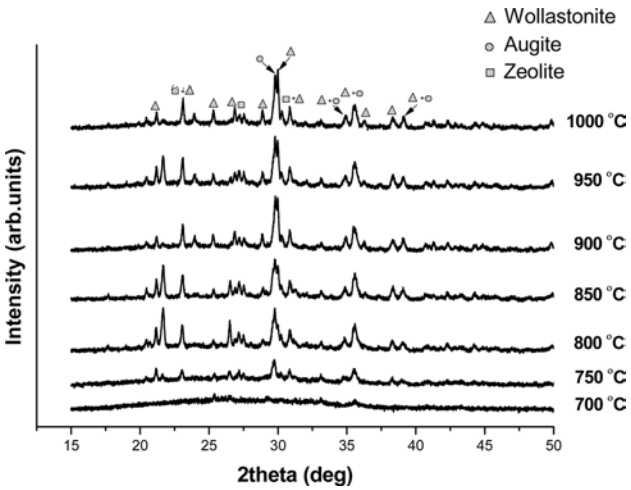

Fig. 1. XRD patterns for the F40 fired at various temperatures.

dominant crystalline phase possessed excellent properties, such as high strength, good chemical resistance, which provide high potential in a wide variety of applications [21].

Characterizations and property testing

Bulk density, porosity, and water absorption, measured according to **ASTM C373-14a**, as a function of the firing temperature of F40, is graphically displayed in Fig. 2(a), (b), and (c) respectively. F40 showed a progressive rate of density development and reached the highest densification (≈ 0.41% water absorption and 0.94%porosity) at 1,000 ºC. The bulk density of the glass-ceramic was around 2.3 g/cm^3 which was close to that of the soda-lime glass.

Fig. 3 shows SEM images of the F40 fired at 900-1,000 ºC. A wide distribution of rod-like crystals on the etched-away glassy phase appeared. The interface showed the presence of smaller size crystals. From the literature, the morphology of monoclinic wollastonite (β-$CaSiO_3$) was rod-like or needle-shaped [22]. It was thus possible that these crystals were wollastonite as agreed with the XRD results.

The Vickers hardness measured using the microhardness indentation technique and the flexural strength for F40 is shown in Fig 4. The error bar shows the standard deviation of five independent samples. The microhardness indentations are of the micrometer-sized scale and have been extensively applied at the microstructure level. With the composite microstructure, however, a great variation of the hardness values could be obtained. The hardness of F40 increased greatly from 2.9 to 7.4 GPa as the sintering temperature was increased from 900 ºC to 1,000 ºC. These obtained values were comparable to hardness values from the two types of floor tiles which were between 272 and 1,115 MPa [23]. The flexural

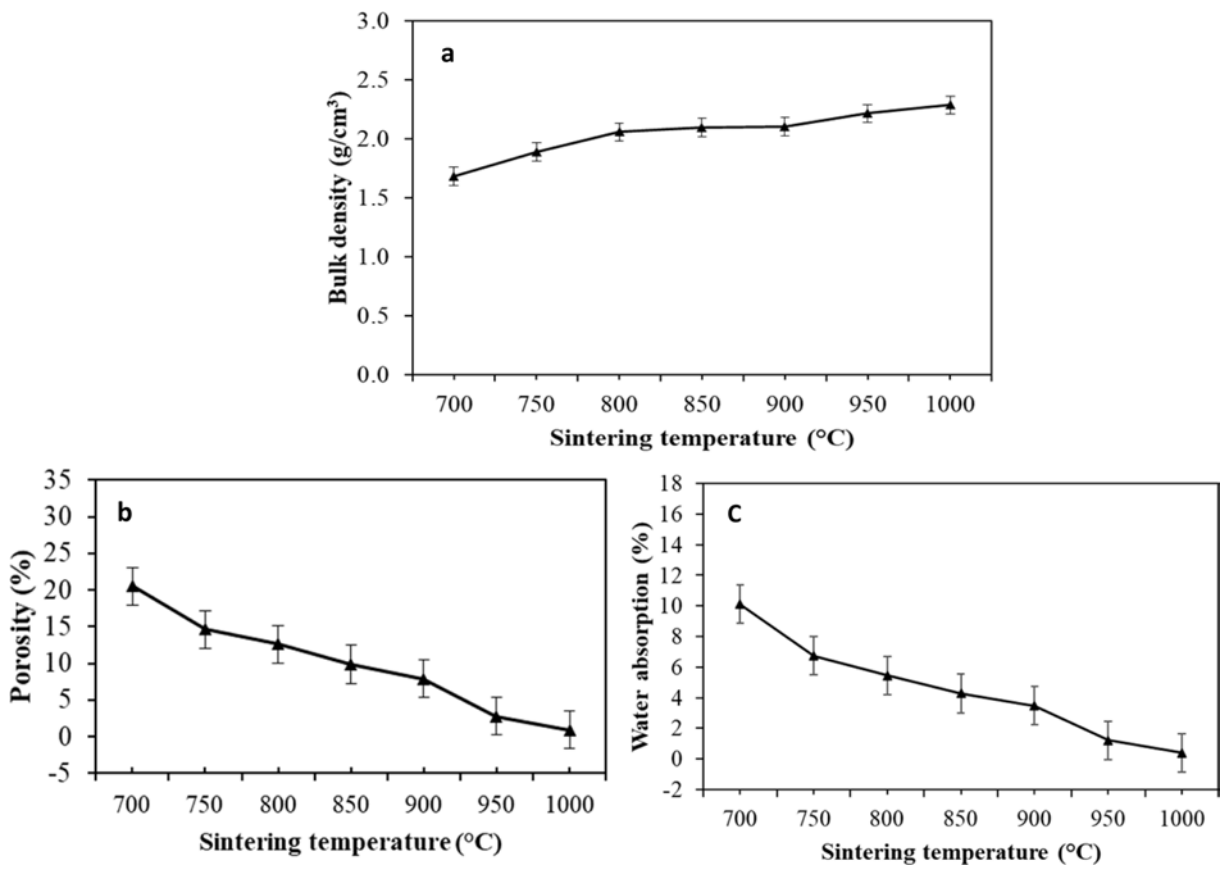

Fig. 2. Physical properties of the F40 fired at various temperatures.

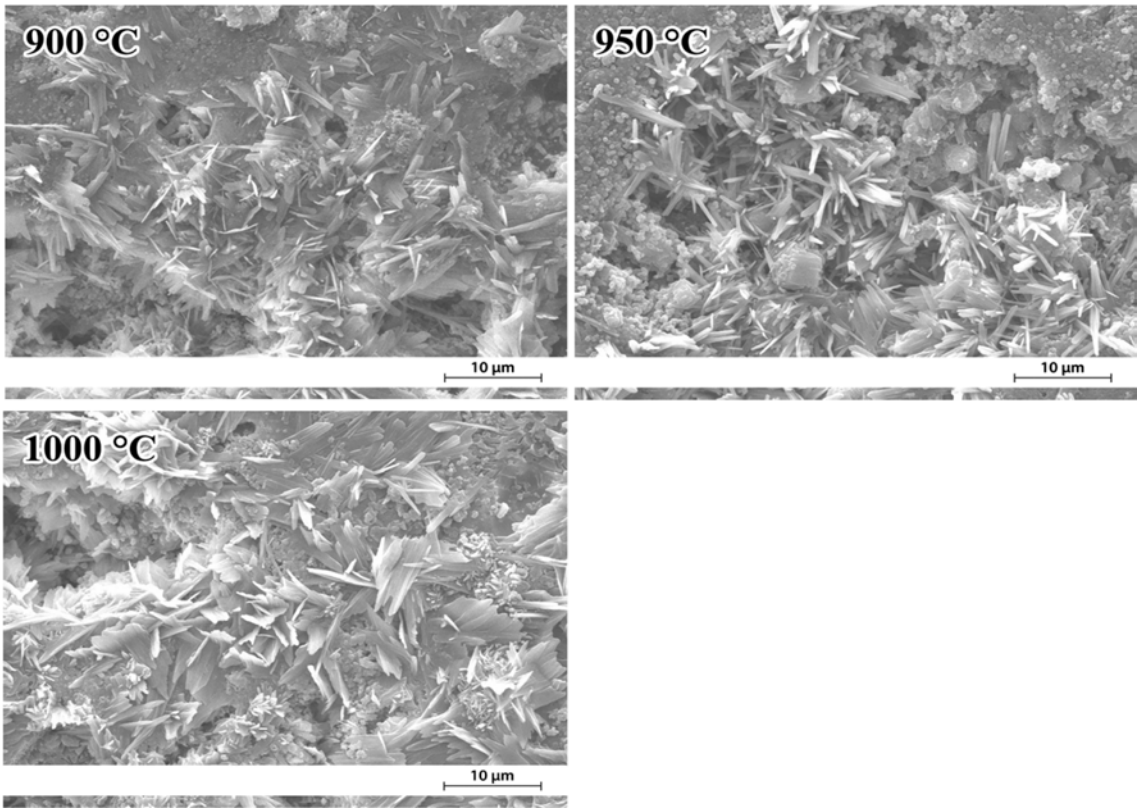

Fig. 3. SEM images of the etched surface of F40 fired at 900-1,000 °C showing the distribution of crystals on the surface.

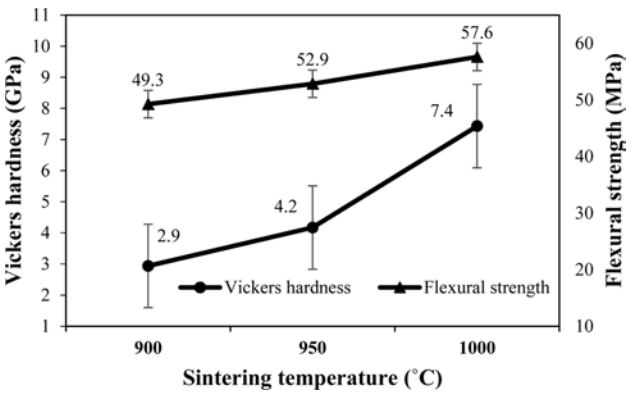

Fig. 4. Variation of the Vickers hardness and flexural strength for the F40 with firing temperatures.

strength of F40 changed from 49.3 to 57.6 MPa with the variation in sintering temperature. Some of the previous work also reported the proximate values of strength [23]. According to the Thai Industrial Standard for Ceramic Tiles (**TIS 2508-2555**), ceramic tile of the low (≤ 3%) and intermediate (3 ≤ E ≤ 10%) water absorption types needs to have the mean modulus of flexural strength of at least 35 and 30 MPa respectively. This result suggested that CAS glass ceramics prepared in our studies at 900 °C to 1,000 °C could be used as both low (≤ 3%) and intermediate (3 ≤ E ≤ 10%) water absorption tiles.

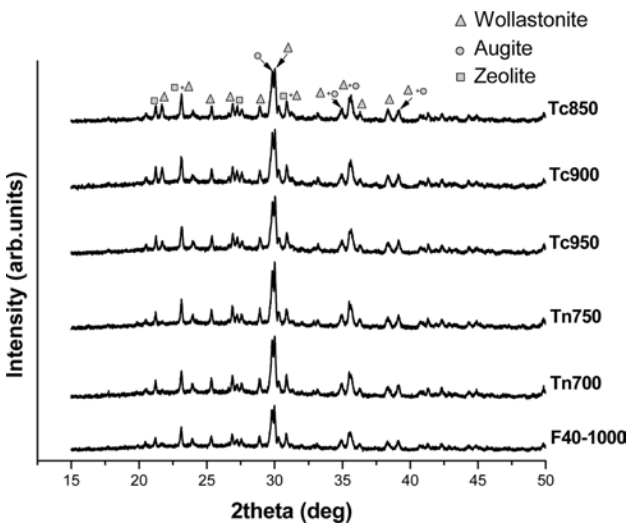

Fig. 5. XRD spectra for the glass-ceramic sintered in different two-stage schemes showing more progressive crystallization in the samples sintered with 2-stage profiles.

Effects of the sintering profile

The XRD spectra for the F40 sintered in two-stage sintering schemes are comparatively shown in Fig. 5. The original F40 sintered in a single stage at 1,000 °C for 1 hr. (F40-1000) is also inserted for comparison. As compared to the F40 which was sintered in a single stage, all samples showed enhancement of the crystallization, i.e. the crystalline peaks were more intensified.

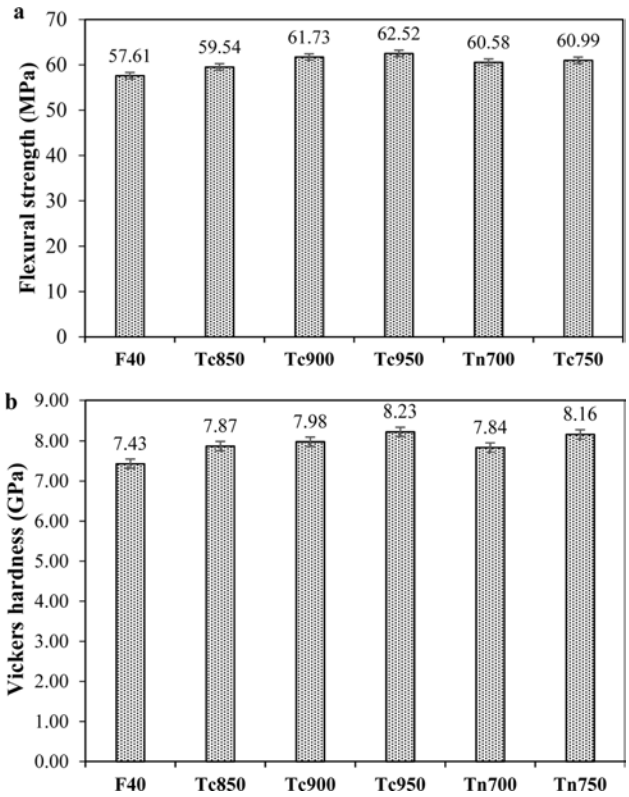

Fig. 6. Variation of and flexural strength Vickers hardness of the glass-ceramics with various sintering schemes.

The effect of the sintering profile on the physical properties of the samples is graphically displayed in Fig. 6. All samples have very close density with a slight variation of porosity and water absorption. All samples showed a water absorption of less than 1% so they can be categorized as the low water absorption tiles.

Vickers hardness and flexural strength of the F40 sintered in the two-stage scheme are graphically shown in Fig. 6. The enhancement of both mechanical properties was observed in all samples. According to the XRD results in Fig. 5, increased crystallinity was observed when the samples were sintered in a two-stage scheme. Based on Griffith's consequence, the possible explanation is when glass-ceramic had more crystals, cracks were difficult to generate or extend [11]. Wollastonite in cement mixtures was reported to moderately improve final compressive strengths and significantly refine flexural toughness, thus enhancing ductility and crack growth resistance [24, 25].

Conclusion

Attempt to prepare CAS glass-ceramics for the construction industry using only waste materials, fly ash, and glass cullet, was achieved. From the results described here, the following conclusions can be drawn:

1) The crystal phases found in F40 were Ca-bearing crystals such as wollastonite, augite, and zeolite being the dominant phases.

2) Vickers hardness values of the F40 were comparable to the values measured from the commercial products.

3) The F40 fired at only 900-1,000 ºC had flexural strength that met the **TIS 2508-2555** standard for the ceramic tile of both low (≤ 3%) and intermediate (3 ≤ E ≤ 10%) water absorption types.

4) Further attempt to enhance the mechanical properties using the 2-stage sintering profile was successful. The maximum Vickers hardness and flexural strength obtained were 8.2 GPa and 62.5 MPa in the Tc950. All these samples have met the **TIS 2508-2555** standard for the ceramic tile of the low (≤ 3%) water absorption types.

Acknowledgment

The authors would like to thank Mae Fah Luang University, Thailand for financial and laboratory support. Support from the Center of Innovative Materials for Sustainability is highly acknowledged.

References

1. R.D. Rawlings, J.P. Wu, and A.R. Boccaccini, J. Mater. Sci. 41 (2006) 733-761.
2. S. Mahdavi, V. Madahi, M. Samedani, and H.R. Rezaie, J. Ceram. Process. Res. 12 (2011) 34-37.
3. J.C.M. Souza, C.S. Silva, J. Caramês, B. Henriques, A.P. Novaes de Oliveira, F.S. Silva, and J.R. Gome, Biotribology. 21 (2020) 100116.
4. S. Papamarkou, C. Sifaki, P.E. Tsakiridis, G. Bartzas, and K. Tsakalakis, J. Environ. Chem. Eng. 6 (2018) 5812-5819.
5. S. Zhao, B. Liu, Y. Ding, J. Zhang, Q. Wen, C. Ekberg, and S. Zhang, J. Clean. Prod. (2020) 122674.
6. G. Sharma and K. Singh, Mater. Chem. Phys. 246 (2020) 122754.
7. P.W. Piché, W.J. O'Brien, C.L. Groh, and K.M. Boenke, Mater. Res. 28 (1994) 603-609.
8. M.Y. Shareef, R. Van Noort, P.F. Messer, and V. Piddock, J. Mater. Sci. Mater. Med. 5 (1994) 113-118.
9. S. Do Yoon and Y.H. Yun, J. Ceram. Process. Res. 12 (2011) 361-364.
10. I. Ponsot, G. Dal Mas, E. Bernardo, R. Dal Maschio, and V.M. Sglavo, J. Ceram. Process. Res. 15 (2014) 411-417.
11. Y. Zhao, D. Chen, Y. Bi, and M. Long, Ceram. Int. 38[3] (2012) 2495-2500.
12. N. Toniolo and A.R. Boccaccini, Ceram. Int. 43[17] (2017) 14545-14551.
13. F.C. Figueira and A.M. Bernardin, J. Alloys Compd. 800 (2019) 525-531.
14. S. Do Yoon, J.U. Lee, J.H. Lee, Y.H. Yun, and W.J. Yoon, J. Mater. Sci. Technol. 29 (2013) 149-153.
15. V. Karayannis, A. Moutsatsou, A. Domopoulou, E. Katsika, C. Drossou, and A. Baklavaridis, J. Build. Eng. 14 (2017) 1-6.
16. J. Temuujin, U. Bayarzul, E. Surenjav, K.D. Sung, and C.Y. Sik, J. Ceram. Process. Res. 18 (2017) 112-115.

17. L.A. Pereira-De-Oliveira, J.P. Castro-Gomes, and P.M.S. Santos, Constr. Build. Mater. 31 (2012) 197-203.
18. N. Pasukphun, A. Hongtong, V. Keawdunglek, Y. Suma, P. Laor, and T. Apidechkul, Appl. Environ. Res. 40 (2018) 55-64.
19. D. Wattanasiriwech, S. Nontachit, P. Manomaivibool, and S. Wattanasiriwech, IOP Conf. Ser.: Earth Environ. Sci. 351 (2019) 012008.
20. S. Wattanasiriwech, F. Arif Nurgesang, D. Wattanasiriwech, and P. Timakul, Ceram. Int. 43[18] (2017) 16055-16062.
21. J. Kang, J. Wang, J. Cheng, J. Yuan, Y. Hou, and S. Qian, J. Non. Cryst. Solids. 457 (2017) 111-115.
22. S. Papamarkou, C. Sifaki, P.E. Tsakiridis, G. Bartzas, and K. Tsakalakis, J. Environ. Chem. Eng. 6 (2018) 5812-5819.
23. L. Sidjanin, D. Rajnovic, J. Ranogajec, and E. Molnar, J. Euro. Ceram. Soc. 27 (2007) 1767-1773.
24. M. Sathiyakumar and F.D. Gnanam, Ceram. Int. 29[8] (2003) 869-873.
25. M. Abdel Wahab, I. Abdel Latif, M. Kohail, A. Almasry, Constr. Build. Mater. 152 (2017) 304-309.